

# Adsorption Thermodynamics and Isotherm Analyses of Cr(VI) Ion from Aqueous Solution Using Low-Cost Adsorbent

<sup>1</sup>R.Sivakumar, <sup>2</sup>S.Arivoli, <sup>3</sup>V.Marimuthu

<sup>1</sup>Assistant Professor, <sup>2</sup>Principal, <sup>3</sup>Guest Lecturer

<sup>1</sup>Department of Chemistry, J.J College of Arts and Science (Autonomous), Pudukkottai, Tamilnadu, India

<sup>2</sup>Department of Chemistry, Poompuhar College, Melaiyur, Nagapattinam, Tamilnadu, India

<sup>3</sup>Department of Chemistry, Thiru.Vi.Ka Govt. Arts College, Thiruvavur, Tamilnadu, India

**Abstract:** The presence of hexavalent chromium Cr(VI) ion in wastewater is a potential hazard to aquatic animals and humans. There are various mechanisms proposed, kinetic models used and adsorption isotherms employed for the efficient removal of hexavalent chromium from industrial and municipal wastewaters using biosorbent. Biosorption of heavy metals is a most promising technology involved in the removal of toxic metals from industrial waste streams and natural waters. Metal removal treatment systems using natural materials are cheap because of the low cost of sorbent materials used and may represent a practical replacement to conventional processes. The work aims at adsorption studies of Cr(VI) ion from aqueous solution onto activated nano carbon prepared from *Syringodium Isoetifolium* Leaves, by acid treatment was tested for its efficiency in removing Cr(VI) ion. The process parameters studied include agitation time, initial chromium ion concentration, adsorbent dose, pH and temperature. The adsorption followed second order reaction equation and the rate is mainly controlled by intra-particle diffusion. The equilibrium adsorption data were correlated with Langmuir, Freundlich, Temkin, Dubinin-Radushkevich, Hurkins-Jura, Halsay, Redlich-Peterson, Jovanovich and BET isotherm models. The influence of pH on Cr(VI) ion removal was significant and the adsorption was increased with increase in temperature. A portion of the Cr(VI) ion was recovered from the spent ASI-NC using 0.1M HCl.

**Index Terms-** Activated *Syringodium Isoetifolium* Leaves Nanocarbon (ASI-NC), Hexavalent chromium, Biosorption, Thermodynamics, Kinetics, Equilibrium models.

## 1. Introduction

Heavy metal pollution of water and water bodies is a serious environmental problem that affects the quality of water. The consequences are decreasing water supply, increase in cost of purification, eutrophication of water bodies and decrease in aquatic production [1]. With potable water essential to life, no where else are these standards more important than the area of water quality. Not only is water essential for life, it has become the primary workhorse of industries around the world as a working fluid, transport medium, heat transfer fluid, cleaning agent, etc. Unfortunately this has often led to the degradation of water quality as harmful effluents are returned to the environment with various contaminants from these processes [2]. One of the most startling groups of water contaminants are those of heavy metals due to their accumulation in biological systems and their toxicity even at relatively low concentrations [3]. Sources of heavy metal water contamination are varied and can be seen in every step of production from mining, purification and processing, to metal

finishing and electroplating, and even end use [4]. Electroplating, the process by which metal is deposited on a surface via an electric current, has been a major contributor to water contamination by a wide variety of heavy Cr(VI) ion. Industry currently treats electroplating wastewater via a lime-soda precipitation technique that, although effective, essentially shifts the problem to large volumes of sludge containing heavy metals [5]. Not only does this method not solve the problem of heavy metal pollution, electroplating industries also must deal with the loss of the useable metal which is becoming increasingly expensive due to a decrease in the quality of metal ores [6]. What is needed is an economical method, not only for the removal of heavy metals from waste water, but also the recovery of these metals.

In the present investigation the adsorption of Chromium ion on activated carbon prepared from *Syngodium Isoetifolium Leaves* Nano Carbon by carbonization with sulphuric acid has been achieved. The kinetic and equilibrium adsorption data obtained were utilized to characterize the sample prepared [7]. The amounts and rates of adsorption of Chromium using above activated carbon from water were then measured. Three simplified kinetic models including pseudo first order, Pseudo second order equations and Elovich equations were used to describe the adsorption process.

## 2. Materials and methods

All the reagents used for the current investigation were of GR grade from Scientific Equipment Company, Trichy, India. Stock solution (1000 mg/L) of Cr(VI) was prepared by dissolving 5.6578g of  $K_2Cr_2O_7$  in double distilled water. The solution was further diluted to the required concentrations before use. Before mixing the adsorbent, the pH of each Cr (VI) solution was adjusted to the required value by 0.1 M NaOH or 0.1 M HCl solution.

### 2.1. Preparation of Adsorbent

The *Syngodium Isoetifolium* Leaves collected from East Coastal area of Nagapattinam district, Tamilnadu was Carbonized with concentrated Sulphuric Acid and washed with water and activated around  $1000^\circ C$  in a muffle furnace for 5 hrs then it was taken out, ground well to fine powder and stored in a vacuum desiccators.



Fig.2.1.Syngodium Isoetifolium Leaves

### 2.2. Adsorbent characterization

Adsorbent characterization was performed by means of spectroscopic and quantitative analysis. The surface area of the adsorbent was determined by Quanta chrome surface area analyzer. The pH of aqueous slurry was determined by soaking 1g of biomass in 50 mL distilled water, stirred for 24 h and filtered and the final pH was measured [9]. The physico-chemical characteristics of the adsorbent were determined using standard procedures [10]. The equilibrium Cr(VI) concentration was

determined by using 1,5-diphenylcarbazide as the complexing agent and a UV-VIS Spectrophotometer (Systronics, Vis double beam Spectro 1203) at a  $\lambda_{\max}$  of 370 nm. For stirring purpose magnetic stirrer was used. The pH of zero-point charge or  $\text{pH}_{\text{ZPC}}$  was determined based on the previous method [9].

Analysis	Value
$\text{pH}_{\text{slurry}}$	6.5400
$\text{pH}_{\text{zpc}}$	6.9000
Moisture content, %	0.1527
Particle density, $\text{g cm}^{-3}$	0.3105
Conductivity, $\mu\text{S/cm}$	32.730
Surface area, $\text{m}^2/\text{g}$	15.200

**Table: 2.1. Physicochemical characteristics of ASI-NC**

### 2.3. Batch Adsorption experiments

The Batch adsorption experiments were conducted in 250 mL Erlenmeyer flask with 50mL of standard Cr(VI) ion solution and were agitated in a thermo state –controlled shaker at 120 rpm. All experiment were conducted at 30-60 °C, unless otherwise was stated.

The effect of initial pH on the adsorption of the Cr(VI) ion onto the activated carbon was studied across a pH range of 2.0 – 9.0 with a fixed adsorbent concentration (25 mg/50ml of  $20\text{mgL}^{-1}$  of Cr(VI) ion solution). The pit value of the initial metal solution ( $50\text{mgL}^{-1}$ ) was adjusted using a 0.1M HCl or NaOH solution. Activated nano carbon (0.0250g) was then added to the solution and agitated for enough time to achieve equilibrium. The effect of the agitation period was also studied at a constant concentration of  $20\text{ mg L}^{-1}$ Cr(VI) ion solution and a fixed adsorbent concentration of 25mg/50mL at the optimum pH. After agitation the sample solution was withdrawn at different time intervals (15-60min) and centrifuged at 1000 rpm for 10 min. Subsequently an aliquot of the supernatant was used for determination of the remaining Cr(VI) ion concentration, and the remainder was poured back into the original solution. The determination of the effect of the initial concentration of the uptake of the Cr(VI) ion was conducted by varying the Cr(VI) ion concentration from 10 to 50  $\text{mg L}^{-1}$  at a constant activated carbon dosage of 25 mg at optimum pH and agitation period. The effect of temperature on the adsorption characteristics was studied by determining the adsorption isotherms from 303 – 333K at a Cr(VI) ion concentration of 10-50mg/L.

The percentage removal of the Cr(VI) ions and the amount of Cr(VI) ion taken up by the adsorbent was calculated by applying following equations.

$$\% \text{ Removal} = \frac{C_i - C_t}{C_i} \times 100 \dots \dots \dots (1)$$

$$Q = \frac{(C_i - C_t)}{m} V \dots \dots \dots (2)$$

Where  $C_i$  and  $C_t$  are the initial and liquid phase concentrations of Cr(VI) at time 't' ( $\text{mg L}^{-1}$ ), Q is the amount of Cr(VI) ion adsorbed on the adsorbate of at any time ( $\text{mg g}^{-1}$ ), m(g) the mass of the adsorbent sample used and V the volume of the Cr(VI) ion solution (L).

### 3. Adsorption of Cr(VI) ions using ASI-NC

#### 3.1. Effect of contact time

The Fig. 3.1 shows that the adsorption of Cr(VI) ion from an aqueous solution reached equilibrium within 45 min. The contact time significantly affected the Cr(VI) ion uptake. The adsorption of Cr(VI) ion by all studied concentrations sharply increased in the first 45 min. The rapid adsorption at the initial stage was probably due to the great concentration gradient between the Cr(VI) ion in solution and the Cr(VI) ion in the adsorbent because there must be a number of vacant sites available in the beginning. The progressive increase in adsorption and consequently, the attainment of equilibrium adsorption is initially due to the limited mass transfer of the Cr(VI) ion from the bulk solution to the external surface of the adsorbent and is subsequently due to the slower internal mass transfer within the adsorbent particles [10].

#### 3.2. Effect of initial Cr(VI) ion concentration

The experimental results of adsorption of Cr(VI) ions on ASI-NC at various initial concentration (10, 20, 30, 40 and 50 mg/L) for chromium ions in terms of equilibrium data are given in table 3.1. The initial concentration provides an important driving force to overcome the mass transfer resistance of all of the molecules between the aqueous and solid phase. While increasing the initial Cr(VI) ion concentration from 10 to 50 mg/L, the percentage of Cr(VI) ion removal by the ASI-NC decreased from 86-75% respectively, the percentage removal of the Cr(VI) ion decreased slowly in the concentration range of 10-50 mg/L, but reduced rapidly from 10 to 30 mg/L Cr(VI) ion removal is highly concentration dependent at higher concentrations. This can be explained by the fact that the adsorbent has a limited number of active sites that become saturated above a certain concentration. At low Cr(VI) ion concentrations, the ratio of surface active sites to the total Cr(VI) ion in the solution is high and hence all Cr(VI) ion may interact with the active pores on the surface of the carbon and be removed from the solution [10-14]. However, with increased Cr(VI) ion concentrations, the number of active adsorption sites is not enough to accommodate the Cr(VI) ion. Therefore, the initial Cr(VI) ion concentration was fixed at 20 mg/L in the following experiments.

#### 3.3. Effect of adsorbent dose

In this study, Five different adsorbent dosages were selected ranging from 0.025 to 0.125 g while the Cr(VI) concentration was fixed at 20 mg/L. The results are presented in Fig. 3.2. It was observed that percentage of Cr(VI) ion removal increased with increase in adsorbent dose. Such a trend is mostly attributed to an increase in the sorptive surface area and the availability of more active binding sites on the surface of the adsorbent. This may be due to the decrease in total adsorption surface area available to Cr(VI) ion resulting from overlapping or aggregation of adsorption sites [14-16]. Thus with increasing adsorbent mass, the amount of Cr(VI) ion adsorbed onto unit mass of adsorbent gets reduced, thus causing a decrease in  $q_e$  value with increasing adsorbent mass concentration. Furthermore maximum Cr(VI) ion removal (85.84%) was recorded by 0.025 g ASI-NC and further increase in adsorbent dose did not significantly change the adsorption yield. This is due to the non-availability of active sites on the adsorbent and establishment of equilibrium between the Cr(VI) ion on the adsorbent and in the solution.



### 3.4. Effect of initial solution pH

The pH of an initial Cr(VI) ion solution exerts profound influence on the adsorptive uptake of adsorbate molecules, presumably due to its influence on the surface properties of the adsorbent and ionization/ dissociation of the adsorbate molecule, Therefore investigation of the effect of pH on the adsorption process is helpful to determine the optimized operational parameters for application and to reveal the adsorption mechanism adsorption of Chromium ion onto ASI-NC was carried out to examine the effect of pH (in a range of 2-9) on the removal of Cr(VI) ion from aqueous solution [10-14]. As seen in Fig 3.3. Cr(VI) ion removal by all studied pH increased gradually with increasing pH, especially between pH 2.0 and 7.0, the maximum removal percentages of Chromium onto ASI-NC at pH<sub>Zpc</sub> were 80 to 85% above this point removal % suddenly decreases due to the occupation OH<sup>-</sup> ions on the surface of ASI-NC.

### 3.5. Effect of other ions

The effect of other ions like Cl<sup>-</sup> on the adsorption process studied at different concentrations. The ions added to 20mg/L of Cr(VI) ion solutions and the contents were agitated for 60 min at 30°C. The results had reveals that low concentration of Cl<sup>-</sup> affect the percentage of adsorption of Cr(VI) ion on ASI-NC, because the interaction of Cl<sup>-</sup> at available sites of adsorbent through competitive adsorption is so effective [14]. The higher concentration of other ion Cl<sup>-</sup> increase the adsorption of Cr(VI) ion. This is so because of the formations of electrical double layer on the surface of the ASI-NC.

### 3.6. Effect of temperature

It is well known that temperature plays an important role in the adsorption process. The Cr(VI) ion removal increase rapidly from 303K to 333K, this result suggests that the experimental temperature had a greater effect on the adsorption process implying that the surface coverage increased at higher temperatures. This may be attributed to the increased penetration of Cr(VI) ion inside enlarged micro pores or the creation of new active sites at higher temperatures. This indicates the endothermic nature of the controlled adsorption process. Similar result has been reported in the literature.

### 3.7. Adsorption isotherm models

Adsorption isotherm [12] describes the relation between the amount or concentration of adsorbate that accumulates on the adsorbent and the equilibrium concentration of the dissolved adsorbate. Equilibrium studies were carried out by agitating a series of beakers containing 50 mL of Cr(VI) solutions of initial concentrations 10-50mg/L with 0.025 g of activated nano carbon at 30-60°C with a constant agitation. Agitation was provided for 1.0 h, which is more than sufficient time to reach equilibrium.

#### 3.7.1. Freundlich adsorption isotherm

The Freundlich adsorption isotherm [15] is based on the equilibrium sorption on heterogeneous surfaces. This isotherm is derived from the assumption that the adsorption sites are distributed exponentially with respect to heat of adsorption.

The adsorption isotherm is expressed by the following equation

$$q_e = K_F C_e^{1/n_F} \dots \dots \dots (3)$$

Which, can be linearized as

$$\ln q_e = \ln K_F + \frac{1}{n_F} \ln C_e \dots \dots \dots (4)$$

Where,  $q_e$  is the amount of MB adsorbed at equilibrium (mg/g) and  $C_e$  is the concentration of Cr(VI) in the aqueous phase at equilibrium (ppm).  $K_F$  (L/g) and  $1/n_F$  are the Freundlich constants related to adsorption capacity and sorption intensity, respectively.

The Freundlich constants  $K_F$  and  $1/n_F$  were calculated from the slope and intercept of the  $\ln q_e$  Vs  $\ln C_e$  plot, and the model parameters are shown in Table 3.2. The magnitude of  $K_F$  showed that ASI-NC had a high capacity for Cr(VI) adsorption from the aqueous solutions studied. The Freundlich exponent,  $n_F$ , should have values in the range of 1 and 10 (i.e.,  $1/n_F < 1$ ) to be considered as favourable adsorption. A  $1/n_F$  value of less than 1 indicated that Cr(VI) is favorably adsorbed by ASI-NC. The Freundlich isotherm did not show a good fit to the experimental data as indicated by SSE and Chi-square statistics.

### 3.7.2. Langmuir adsorption isotherm

The Langmuir adsorption isotherm [16] is based on the assumption that all sorption sites possess equal affinity to the adsorbate. The Langmuir isotherm [14] in a linear form can be represented as:

$$\frac{C_e}{q_e} = \frac{1}{q_m K_L} + \frac{C_e}{q_m} \dots \dots \dots (5)$$

Where,  $q_e$  is the amount of Cr(VI) adsorbed at equilibrium (mg/g),  $C_e$  is the concentration of Cr(VI) in the aqueous phase at equilibrium (ppm),  $q_m$  is the maximum Cr(VI) uptake (mg/g), and  $K_L$  is the Langmuir constant related to adsorption capacity and the energy of adsorption (g/mg). A linear plot of  $C_e/q_e$  Vs  $C_e$  was employed to determine the value of  $q_m$  and  $K_L$  and the data so obtained were also presented in Table 3.2. The model predicted a maximum value that could be reached in the experiments. The value of  $K_L$  decreased with an increase in the temperature. A high  $K_L$  value indicates a high adsorption affinity. The dimensionless constant separation factor or equilibrium parameter ( $R_L$ ) defined in the following equation:

$$R_L = \frac{1}{1 + K_L C_0} \dots \dots \dots (6)$$

Where,  $C_0$  is the initial Cr(VI) concentration (ppm). Four scenarios can be distinguished: The sorption isotherm is unfavorable when  $R_L > 1$ , the isotherm is linear when  $R_L = 1$ . The isotherm is favorable when  $0 < R_L < 1$  and the isotherm is irreversible when  $R_L = 0$ . The value of  $Q_m$  decreased with an increase in the temperature shows the adsorption efficiency of ASI-NC at low temperature is so effective. A high  $b$  value indicates a high adsorption affinity. The values of dimensionless separation factor ( $R_L$ ) for Cr(VI) removal were calculated at different concentrations and temperatures. As shown in Table 3.3, at all concentrations and temperatures tested the values of  $R_L$  for Cr(VI) adsorptions on the ASI-NC were less than 1 and greater than zero, indicating favorable adsorption. The Langmuir isotherm showed a better fit to the adsorption data than the Freundlich

isotherm. The fact that the Langmuir isotherm fits the experimental data well may be due to homogeneous distribution of active sites on the ASI-NC surface, since the Langmuir equation assumes that the adsorbent surface is energetically homogeneous [17].

**3.7.3. Temkin adsorption isotherm**

The Temkin adsorption isotherm [18, 19] assumes that the heat of adsorption decreases linearly with the sorption coverage due to adsorbent-adsorbate interactions. The Temkin isotherm equation is given as:

$$q_e = \frac{RT}{bT} \ln K_T + \frac{RT}{bT} \ln C_e \dots \dots \dots (7)$$

Which, can be represented in the following linear form

$$q_e = \frac{RT}{bT} \ln(K_T C_e) \dots \dots \dots (8)$$

Where,  $K_T$  (L/g) is the Temkin isotherm constant,  $b_T$  (J/mol) is a constant related to heat of sorption,  $R$  is the ideal gas constant (8.314 J/mol K), and  $T$  is absolute temperature (K). A plot of  $q_e$  versus  $\ln C_e$  enables the determination of isotherm constants  $K_T$  and  $b_T$  from the slope and intercept. The model parameters are listed in Table 3.2. The Temkin isotherm appears to provide a good fit to the Cr(VI) adsorption data. The adsorption energy in the Temkin model,  $b_T$ , is positive for Cr(VI) adsorption from the aqueous solution, which indicates that the adsorption is endothermic. The experimental equilibrium curve is close to that predicted by Temkin model.

**3.7.4. Hurkins-Jura adsorption isotherm**

The Hurkins-Jura adsorption isotherm can be expressed as [20]

$$q_e = \sqrt{\frac{A_H}{B_H + \log C_e}} \dots \dots \dots (9)$$

This can rearranged as follows:

$$\frac{1}{q_e^2} = \frac{B_H}{A_H} - \frac{1}{A_H} \log C_e \dots \dots \dots (10)$$

Where,  $A_H$  ( $g^2/L$ ) and  $B_H$  ( $mg^2/L$ ) are two parameters characterizing the sorption equilibrium. The Hurkins-Jura adsorption isotherm accounts for multilayer adsorption and can be explained by the existence of a heterogeneous pore distribution. The Harkins–Jura isotherm parameters are obtained from the plots of  $1/q_e^2$  versus  $\log C_e$  enables the determination of model parameters  $A_H$  and  $B_H$  from the slope and intercept. The obtained values from the graph are listed in Table 3.2 attest to the heteroporous nature of the adsorbent which makes multilayer physical adsorption i.e., one may through pores another may be on the surface

**3.7.5. Halsay adsorption isotherm**

The Halsay adsorption isotherm can be give as [21]

$$q_e = \exp\left(\frac{\ln K_{H_a} - \ln C_e}{n H_a}\right) \dots \dots \dots (11)$$

And, a linear form of the isotherm can be expressed as follows:

$$\ln q_e = \frac{\ln K_{H_a}}{n H_a} - \frac{\ln C_e}{n H_a} \dots \dots \dots (12)$$

Where,  $K_{Ha}$  (mg/L) and  $n_{Ha}$  are the Halsay isotherm constants. A plot of  $\ln q_e$  Vs  $\ln C_e$ . This one enables the determination of  $n_{Ha}$  and  $K_{Ha}$  from the slope and intercept. This equation is suitable for multilayer adsorption and the fitness of the experimental data to this equation attests the heteroporous nature of adsorbent. The model parameters are listed in Table 3.2. The obtained result also shows that the adsorption of Cr(VI) on ASI-NC was not based on significant multilayer adsorption. The Halsay model is also not suitable to describe the adsorption of Cr(VI) on ASI-NC, because this model also assumes a multilayer behavior for the adsorption of adsorbate onto adsorbent.

**3.7.6. Redlich-Peterson adsorption isotherm**

The Redlich-Peterson adsorption isotherm contains three parameters and incorporates the features of Langmuir and Freundlich isotherms into a single equation. The general isotherm equation can be described as follows [22]

$$q_e = \frac{K_R C_e}{1 + aR C_e^g} \dots \dots \dots (13)$$

The linear form of the isotherm can be expressed as follows:

$$\ln q_e = \frac{K_R C_e}{1 + aR C_e^g} \dots \dots \dots (14)$$

Where,  $K_R$  (L/g) and  $a_R$  (L/mg) are the Radlich-Peterson isotherm constants and  $g$  is the exponent between 0 and 1. There are two limiting cases: Langmuir form for  $g = 1$  and Henry’s law for  $g = 0$ . A plot of  $\ln C_e/q_e$  versus  $\ln C_e$  enables the determination of isotherm constants  $g$  and  $K_R$  from the slope and intercept. The values of  $K_R$ , presented in Table 3.2, indicate that the adsorption capacity of the ASI-NC decreased with an increase temperature. Furthermore, the value of  $g$  lies between 0 and 1, indicating the favorable adsorption.

**3.7.7. Dubinin-Radushkevich adsorption isotherm**

The Dubinin-Radushkevich adsorption isotherm [23] is another isotherm equation. It is assumed that the characteristic of the sorption curve is related to the porosity of the adsorbent. The linear form of the isotherm can be expressed as follows

$$\ln q_e = \ln Q_D - B_D \left[ RT \ln \left( 1 + \frac{1}{C_e} \right) \right]^2 \dots \dots \dots (15)$$

Where,  $Q_D$  is the maximum sorption capacity (mol/g), and  $B_D$  is the Dubinin-Radushkevich constant (mol<sup>2</sup>/kJ<sup>2</sup>). A plot of  $\ln q_e$  Vs  $RT \ln(1+1/C_e)$  enables the determination of isotherm constants  $B_D$  and  $Q_D$  from the slope and intercept. A plot of  $\ln q_e$  Vs  $RT \ln(1+1/C_e)$  enables the determination of isotherm constants  $B_D$  and  $Q_D$  from the slope and intercept as shown in Table 3.2. The adsorption data’s are well correlated with this model suggesting the possibility of heterogeneous pores on ASI-NC [24].

**3.7.8. Jovanovich adsorption isotherm**

The equilibrium data were analyzed with Jovanovich adsorption isotherm [25] model for removal of Cr(VI). . The Jovanovic model leads to the following relationship

$$q_e = q_{max} (1 - e^{-K_j C_e}) \dots \dots \dots (16)$$

The linear form of the isotherm can be expressed as follows:



$$\ln q_e = \ln q_{\max} - K_J C_e \dots \dots \dots (17)$$

Where,  $K_J$  (L/g) is a parameter.  $q_{\max}$  (mg/g) is the maximum Cr(VI) uptake. The assumptions of Jovanovich isotherm model corresponds to another approximation for monolayer localized adsorption without lateral interactions. This model is similar to that of Langmuir model except that the allowance is made in the former for the surface binding vibrations of an adsorbed species. The Jovanovich adsorption isotherm parameters are obtained from the plot of  $\ln q_e$  and  $C_e$  are listed in Table 3.2. The calculated  $q_{\max}$  and  $K_J$  results show that the accordance of the Jovanovich model with the Langmuir and Temkin models for the Cr(VI) adsorption by ASI-NC. The model shows a high degree of correlation.

### 3.7.9. The Brunauer-Emmett-Teller (BET) isotherm model

Brunauer-Emmett-Teller (BET) isotherm [26] is a theoretical equation, most widely applied in the gas–solid equilibrium systems. It was developed to derive multilayer adsorption systems with relative concentration ranges from 0.1 to 0.50 corresponding to a monolayer coverage lying between 0.50 and 1.50.

Its extinction model related to liquid–solid interface is exhibited as:

$$q_e = \frac{q_s C_{\text{BET}} C_e}{(C_s - C_e) \left[ 1 + (C_{\text{BET}} - 1) \left( \frac{C_e}{C_s} \right) \right]} \dots \dots \dots (18)$$

Where,  $C_{\text{BET}}$ ,  $C_s$ ,  $q_s$  and  $q_e$  are the BET adsorption isotherm (L/mg), adsorbate monolayer saturation concentration (mg/L), theoretical isotherm saturation capacity (mg/g) and equilibrium adsorption capacity (mg/g), respectively. As  $C_{\text{BET}}$  and  $C_{\text{BET}} (C_e/C_s)$  is much greater than 1,

In the linear form as used is represented as

$$\frac{C_e}{q(C_s - C_e)} = \frac{1}{q_s C_{\text{BET}}} + \left( \frac{C_{\text{BET}} - 1}{q_s C_{\text{BET}}} \right) \left( \frac{C_e}{C_s} \right) \dots \dots \dots (19)$$

Where,  $C_e$  is equilibrium Concentration (mg/l),  $C_s$  is adsorbate monolayer saturation concentration (mg/l) and  $C_{\text{BET}}$  is BET adsorption relating to the energy of surface interaction (l/mg). The BET adsorption isotherm parameters are obtained from the slope and intercept of the plot,  $C_e/q_e (C_s - C_e)$  Vs  $C_e/C_s$ . The obtained  $C_{\text{BET}}$  and  $q_s$  results are listed in Table 3.2. The results predict the monolayer coverage of adsorbate on the ASI-NC adsorbent.

### 3.8. Kinetic parameters

The rate and mechanism of the adsorption process can be elucidated based on kinetic studies. Cr(VI) adsorption on solid surface may be explained by two distinct mechanisms: (1) An initial rapid binding of Cr(VI) molecules on the adsorbent surface; (2) relatively slow intra-particle diffusion. To analyze the adsorption kinetics of the Cr(VI), the pseudo-first-order, the pseudo-second-order, and intra-particle diffusion models were applied. Each of these models and their linear modes of them equations presented in below.

## Kinetic Models and Their Linear Forms

Model	Nonlinear Form	Linear Form	Number of Equation
<b>Pseudo-first-order</b>	$dq_t/dt = k_1(q_e - q_t)$	$\ln(q_e - q_t) = \ln q_e - k_1 t$	(20)
<b>Pseudo-second-order</b>	$dq_t/dt = k_2(q_e - q_t)^2$	$t/q_t = 1/k_2 q_e^2 + (1/q_e)t$	(21)

Where,  $q_e$  and  $q_t$  refer to the amount of Cr(VI) adsorbed (mg/g) at equilibrium and at any time,  $t$  (min), respectively and  $k_1$  (1/min),  $k_2$  (g/mg.min) are the equilibrium rate constants of pseudo-first order and pseudo-second order models, respectively. Pseudo-first order model [27] is a simple kinetic model, which was proposed by Lagergren during 1898 and is used for estimation of the surface adsorption reaction rate. The values of  $\ln(q_e - q_t)$  were linearly correlated with  $t$ . The plot of  $\ln(q_e - q_t)$  vs.  $t$  gives a linear relationship from which the values of  $k_1$  were determined from the slope of the plot. In many cases, the first-order equation of Lagergren does not fit well with the entire range of contact time and is generally applicable over the initial stage of the adsorption processes. In the pseudo-second order model [28], the slope and intercept of the  $t/q_t$  Vs  $t$  plot were used to calculate the second-order rate constant,  $k_2$ . The values of equilibrium rate constant ( $k_2$ ) are presented in Table 3.4. According to Table 3.4, the obtained value of  $r^2$  (0.999) reveals the pseudo-second order kinetics of Cr(VI) ions adsorption.

### 3.8.1. Simple Elovich Model

The simple Elovich model [29] is expressed in the form,

$$q_t = \alpha + \beta \ln t \dots\dots\dots(22)$$

Where,  $q_t$  is the amount adsorbed at time  $t$ ,  $\alpha$  and  $\beta$  are the constants obtained from the experiment. A plot of  $q_t$  against  $\ln t$  should give a linear relationship for the applicability of the simple Elovich kinetic. The Elovich kinetics of Cr(VI) on to KASNC for various initial concentrations (10, 20, 30, 40 and 50 mg/L) of volume 50 mL (each), adsorbent dose 0.025g, temperature 28 °C and pH 6.0.

Since, Cr (VI) ions adsorption fits with the Elovich model, a plot of  $q_t$  vs.  $\ln(t)$  yields a linear relationship with a slope of  $(1/\beta)$  and an intercept of  $(1/\beta)\ln(\alpha\beta)$ . The obtained Elovich model parameters  $\alpha$ ,  $\beta$ , and correlation coefficient ( $\gamma$ ) are summarized in Table 3.4. The experimental data such as the initial adsorption rate ( $\alpha$ ) adsorption constant ( $\beta$ ) and the correlation co-efficient ( $\gamma$ ) calculated from this model indicates that the initial adsorption ( $\alpha$ ) increases with temperature similar to that of initial adsorption rate ( $h$ ) in pseudo-second-order kinetics models. This may be due to increase the pore or active site on the ASI-NC adsorbent [30].

### 3.8.2. The Intra-particle diffusion model

The kinetic results were analyzed by the Intra-particle diffusion model [31] to elucidate the diffusion mechanism. . The model is expressed as:

$$q_t = K_{id} t^{1/2} + I \dots\dots\dots(23)$$

Where  $I$  is the intercept and  $K_{id}$  is the intra-particle diffusion rate constant. The intercept of the plot reflects the boundary layer effect. Larger the intercept, greater is the contribution of the surface sorption in the rate controlling step. The calculated diffusion coefficient  $K_{id}$  values are listed in Table 3.4. The  $K_{id}$  value was higher at the higher concentrations. Intra-particle diffusion is the sole rate-limiting step since the regression of  $q_t$  versus  $t^{1/2}$  is linear and passes through the origin. In fact, the linear plots at each concentration never pass through the origin. This deviation from the origin is due to the difference in the rate of mass transfer in the initial and final stages of the sorption. This one indicates the existence of some boundary layer effect and further showed that Intra-particle diffusion was not the only rate-limiting step.

It is clear from the Table 3.4 that the pseudo- second-order kinetic model showed excellent linearity with high correlation coefficient ( $r^2 > 0.99$ ) at all the studied concentrations in comparison to the other kinetic models. In addition the calculated  $q_e$  values also agree with the experimental data in the case of pseudo-second-order kinetic model. It is also evident from Table 3.4 that the values of the rate constant  $k_2$  decrease with increasing initial Cr(VI) concentrations. This is due to the lower competition for the surface active sites at lower concentration but at higher concentration the competition for the surface active sites will be high and consequently lower sorption rates are obtained.

### 3.9 Adsorption Thermodynamics

#### 3.9.1 Thermodynamic parameters

Thermodynamic parameters [32-35] were evaluated to confirm the adsorption nature of the present study. The thermodynamic constants, free energy change, enthalpy change and entropy change were calculated to evaluate the thermodynamic feasibility and the spontaneous nature of the process. Enthalpy change ( $\Delta H$ ), and entropy change ( $\Delta S$ ) may be determined from Van't Hoff equation:

$$\ln K = \frac{\Delta S}{R} - \frac{\Delta H}{RT} \dots \dots \dots (24)$$

By plotting  $\ln K$  as ordinate and  $1/T$  as abscissa, we will get  $\Delta S$ ,  $\Delta H$  and by using the following equation. We can get the value of have  $\Delta S$ ,  $\Delta H$  and by this equation, get the value of  $\Delta G$ .

$$\Delta G = \Delta H - T\Delta S \dots \dots \dots (25)$$

Where,  $\Delta G$  is the free energy change ( $\text{kJ mol}^{-1}$ ),  $R$  is the universal gas constant ( $8.314 \text{ J mol}^{-1} \text{ K}^{-1}$ ),  $K$  the thermodynamic equilibrium constant and  $T$  is the absolute temperature (K).

$$\Delta G = \Delta H - T\Delta S = -RT \ln K_c \dots \dots \dots (26)$$

$$\ln K_c = \frac{\Delta S}{R} - \frac{\Delta H}{RT} \dots \dots \dots (27)$$

$$2.303 \log \frac{q_e}{C_e} = \frac{\Delta S}{R} - \frac{\Delta H}{RT} \dots \dots \dots (28)$$

$$\log \frac{q_e}{C_e} = \frac{\Delta S}{R \times 2.303} - \frac{\Delta H}{RT \times 2.303} \dots \dots \dots (29)$$

The values of  $\Delta S^\circ$ ,  $\Delta H^\circ$ ,  $\Delta G^\circ$  was obtained from a plot of  $\ln K_c$  vs.  $1/T$ . The value of  $\Delta H^\circ$  range from 3 to 22 kJ/mol from Table 3.5 which indicate that the nature of adsorption of Cr(VI) on ASI-NC is by physical adsorption. The negative value of  $\Delta G^\circ$  indicate the spontaneous process of adsorption of Cr(VI) on ASI-NC. The positive value of  $\Delta S^\circ$  reflects the affinity of the adsorbent for the adsorption of Cr(VI) because the collision between the Cr (VI) and ASI-NC surface is more effective that leads to the randomness on the surface. The values of  $E_a$  and  $S^*$  can be calculated from slope and intercept of the plot of  $\ln(1-\theta)$  versus  $1/T$  respectively and are listed in Table 3.5. The result as shown in Table 3.5 indicate that the probability of the Cr(VI) to stick on surface of biomass is very high as  $S^* \ll 1$ , these values confirm that, the sorption process is physisorption [33-36].

### 3.10 Desorption studies

In order to assess the reusability of chromium loaded ASI-NC biomass. The desorption experiments were carried out with various very dilute acidic and basic solutions. The effect of strength of desorbing solution (NaOH) on the recovery of Cr(VI) ion. When the strength of the desorbing solution increased from 0.5 to 2.0 M, Cr (VI) desorption percentage increased from 28.5% to 79%. The very dilute HCl is so effective in the removal loaded Cr(VI) from ASI-NC, which shows that the ASI-NC biomass can be effectively reused after desorption as well as it confirms the physisorption of Cr(VI) on ASI-NC [34].

### 4. Conclusion

ASI-NC prepared from *Syringodium Isoetifolium* Leaves was found effective in removing Cr(VI) ion from aqueous solution. The adsorption is faster and the rate is mainly controlled by intra-particle diffusion. Using the sorption equation obtained from the Langmuir and Freundlich isotherms, it was found that ASI-NC is an effective one for the removal of Cr(VI) ion. The adsorption kinetic process was found pseudo-second order model. Isotherm and kinetic study indicates that the ASI-NC can be effectively employed for the adsorption of Cr(VI) ions. Thermodynamic results show that adsorption of Cr(VI) ions on to ASI-NC was spontaneous and physical adsorption.

### References

- [1] K.Al-Sou'od, Adsorption kinetics for the removal of hexavalent chromium using low cost materials, *Research Journal of Chemistry and Environment*, 17,25-30,(2013).
- [2] Indian Standard, Drinking Water-Specification (First revision), IS10500, 1991.
- [3] EPA, (Environmental Protection Agency), Environmental Pollution Control Alternatives, 1990, EPA/625/5-90/025, EPA/625/4-89/023, Cincinnati, US.
- [4] F.Boudrahem, A.Soualah, F.Aissani-Benissad, Pb(II) and Cd(II) removal from aqueous solutions using activated carbon developed from coffee residue activated with phosphoric acid and zinc chloride, *Journal of Chemical & Engineering Data* 56,1946-1955, (2011).
- [5] F. Mohammed-Azizi, S. Dib, M. Boufatit, Removal of heavy metals from aqueous solutions by Algerian bentonite. *Desalination and Water Treatment*. 51, 4447-4458, (2013)

- [6] R S.Juang R C.Shaiu.Metal removal from aqueous solutions using chitosan enhanced membrane filtration, *Journal of Membrane Science*. 165,59-167,(2000).
- [7] G.Yan. T. Viraraghavan. Heavy metal removal in a biosorption column by immobilized *M.rouxii* biomass. *Bioresource Technology*. 78(3), 243-249, (2001).
- [8] K.Y.Foo. B.H. Hameed. Insights into the modeling of adsorption isotherm system, *Chemical Engineering Journal*. 156 (1),2-10, (2010).
- [9] Brown, P., Jefcoat, I., Parrish, A., Dana, G., Sarah, S. and Graham, E, Evaluation of the adsorptive capacity of peanut hull pellets for heavy metals in solution. *Advanced in Environmental Research*. 4(1),19-29,( 2000)
- [10] Shrivastava, R.K., Ayachi, A.K. and Mora, M. Removal of Cr (VI) by utilization of Bidi leaves. *Pollution Research*. 20(4),639 – 643, ( 2001)
- [11] Namasivayam, C. and Holl, W.H, Chromium (III) removal in tannery wastewaters using Chinese reed (*MiscanthusSinensis*), a fast growing plant. *Holz. Roh. Werkst*. 62, 74 – 80, (2004).
- [12] Vadivelan V, Kumar K V., Equilibrium, kinetics, mechanism and process design for the sorption of methylene blue onto rice husk, *Journal of Colloid and Interface Science*., 286, 90-100, (2005)
- [13] Arivoli S, Viji Jain M, Rajachandrasekar T., Cobalt adsorption on a low cost carbon-kinetic, equilibrium and mechanistic studies, *Material Science Research India*, 3 241-250,(2006).
- [14] Namasivayam C, Jeyakumar R, Yamuna R T and Jayanthi J., Dye removal from wastewater by adsorption on 'waste' Fe(III)/Cr(III) hydroxide, *Waste Management*., 14, 643-648, (1994).
- [15] Arivoli S, Venkatraman B R, Rajachandrasekar T, Hema M., Adsorption of ferrous ion from aqueous solution by acid activated low cost carbon obtained from natural plant material, *Research Journal of Chemistry and Environment*., 17,70-78, (2007).
- [16] Langmuir I., *Journal of American Society*. 579, 1361-1403, (1918).
- [17] Namasivayam C, Yamuna R T., Adsorption of direct red 12 B by biogas residual slurry: Equilibrium and rate processes, *Environment Pollution*., 89, 1-7, (1995).
- [18] Rao GB, Kalyani G., Saradhi BV and Kumar YP., Removal of Fluoride from Aqueous solution using a waste Material., *Nature Environment Pollution Technology*., 8(2), 231, (2009).
- [19] Temkin M J and Pyzhev V., *Acta Physiochim USSR*., 12, 217-222, (1940)
- [20] Abdelwahab O., Evaluation of the use of loofa activated carbons as potential adsorbents for aqueous solutions containing dye., *Desalination*., 222(1), 357-367, (2008).
- [21] Ng C., Losso JN., Marshall WE, Rao RM., *Bioresource Technology*., Freundlich adsorption isotherms of agricultural by-product-based powdered activated carbons in a geosmin-water system. 85(2), 131-5, (2002).
- [22] Akbal F., Adsorption of basic dyes from aqueous solution onto pumice powder. *Journal of Colloid and Interface Science*., 286(2), 455-8. (2005).
- [23] Dubinin M M., The Potential Theory of Adsorption of Gases and Vapors for Adsorbents with Energetically Non-Uniform Surface, *Chemical Reviews*, 60, 235-266, (1960).
- [24] Dubinin M M., Modern State of the Theory of Volume Filling of Micropore Adsorbents during



- Adsorption of Gases and Steams on Carbon Adsorbents. *Zhurnal Fizicheskoi Khimii*, 39, 1305-1317, (1965).
- [25] Asgari G, Roshani B and Ghanizadeh G., The investigation of kinetic and isotherm of fluoride adsorption onto functionalize pumice stone, *Journal of Hazardous Matter*, 217-218, 123-32, (2012)
- [26] Mahvi A H, Heibati B, Mesdaghinia A, Yari A R., Fluoride Adsorption by Pumice from Aqueous solutions., *Journal of Chemistry*, 9(4), 1843-1853, (2012).
- [27] Colak F, Atar N and Olgun A., Biosorption of acidic dyes from aqueous solution by *Paenibacillus macerans*: Kinetic, thermodynamic and equilibrium studies, *Chemical Engineering Journal*, 150(1), 122-30, (2009).
- [28] Mall ID, Srivastava V C and Agarwal NK., Removal of orange-G and methyl violet dyes by adsorption onto bagasse fly ash-kinetic study and equilibrium isotherm analyses, *Dyes and Pigment.*, 69(3), 210-23, (2006).
- [29] Chien S H and Clayton W R., Application of Elovich Equation to the Kinetics of Phosphate Release and Sorption in Soils., *Journal of Soil Science Society of America*, 44, 265-268, (1980).
- [30] Amin N K., Removal of direct blue-106 dye from aqueous solution using new activated carbons developed from pomegranate peel: adsorption equilibrium and kinetics, *Journal of Hazardous Matter*, 165(1- 3), 52-62, (2009)
- [31] Weber W J, Morris J C., Kinetics of Adsorption of Carbon from Solution, *Journal of Sanitary Engineering Division, American Society of Civil Enineering*, 89(17), 31-60,(1963).
- [32] Singh I B and Singh D R., Hexavalent chromium removal using iron bearing industrial sludges, *Indian Journal of Chemical Technology*, 8, 487-495, (2001).
- [33] Volesky B., Sorption and Biosorption, *BV Sorbex, Inc., Montreal*, 316, (2003).
- [34] Albero A S, Albero J S, Escribano A S and Reinoso F R., Ethanol removal using activated carbon: Effect of porous structure and surface chemistry, *Microporous and Mesoporous Materials*, 120, 62-68, (2009).
- [35] Anfruns A, Martin M J and Mones-Moran M A., "Removal of odourous VOCs using sludge-based adsorbents" *Chemical Engineering Journal*, 166, 1022-1031, (2011).
- [36] Aribike D S and Olafadehan O A., Modeling of fixed bed adsorption of phenols on granular activated carbon, *Theoretical Foundations of Chemical Engineering*, 42, 257-263, (2008).

Table: 3.1 Equilibrium Parameters for the Adsorption of Cr (VI) ion onto ASI-NC

M <sub>0</sub>	Ce (mg / L)				Qe (mg / g)				Removed (%)			
	30 °C	40 °C	50°C	60 °C	30 °C	40 °C	50 °C	60 °C	30 °C	40 °C	50 °C	60 °C
10	1.908	1.408	1.158	1.133	16.184	17.184	17.682	17.733	80.918	85.918	88.412	88.667
20	3.408	3.159	2.918	2.408	33.184	33.681	34.163	35.182	82.959	84.203	85.406	87.956
30	6.678	6.109	5.408	5.059	46.642	47.781	49.183	49.881	77.737	79.636	81.972	83.136
40	9.429	8.679	8.266	7.795	61.142	62.641	63.466	64.410	76.427	78.302	79.333	80.512
50	13.65	13.20	12.93	12.20	72.684	73.586	74.139	75.597	72.684	73.586	74.139	75.597

Table: 3.2 Isotherm Parameters for the Adsorption of Cr (VI) ion onto ASI-NC

Model	Constant	Temperature (° C)			
		30	40	50	60
Freundlich	K <sub>f</sub> (mg/g) (L/mg) <sup>1/n</sup>	11.3793	14.6326	17.0348	18.2519
	N	1.35494	1.53307	1.65486	1.66409
Langmuir	Q <sub>m</sub> (mg/g)	148.888	121.252	110.556	110.822
	b (L/mg)	0.07140	0.11679	0.15700	0.17476
Temkin	b <sub>T</sub> (J/mol)	28.0692	25.2895	23.7940	24.2211
	K <sub>T</sub> (L/mg)	0.97277	1.06301	1.10887	1.12809
Hurkins-Jura	A <sub>H</sub> (g <sup>2</sup> /L)	-259.43	-314.592	-354.117	-369.335
	B <sub>H</sub> (mg <sup>2</sup> /L)	-1.0423	-1.02247	-1.00519	-0.97868
Halsay	K <sub>Ha</sub> (mg/L)	26.9756	61.1671	109.0662	125.5837
	n <sub>Ha</sub>	1.35494	1.53307	1.65486	1.66409
Radlich-Peterson	G	0.26196	0.34771	0.39572	0.39907
	K <sub>R</sub> (L/g)	0.08788	0.06834	0.05870	0.05479
Dubinin-Radushkevich	q <sub>s</sub> (mg/g)	63.5060	60.6256	60.2518	63.4980
	K <sub>D</sub> × 10 <sup>-4</sup> mol <sup>2</sup> kJ <sup>-2</sup>	1.48941	1.47262	1.46680	1.47621
Jovanovic	K <sub>J</sub> (L/g)	0.11479	0.11349	0.11112	0.11586
	q <sub>max</sub> (mg/g)	18.1765	19.9570	21.5254	22.3003
BET	C <sub>BET</sub> (L/m)	4.47133	6.22881	8.72294	10.08890
	q <sub>s</sub> (mg/g)	0.22365	0.16054	0.11464	0.09912

Table: 3.3 Dimensionless Separation factor (R<sub>L</sub>) for the Adsorption of Cr (VI) ion onto ASI-NC

(C <sub>i</sub> )	TEMPERATURE °C			
	30°C	40°C	50°C	60°C
10	0.3591	0.2551	0.2030	0.1863
20	0.2188	0.1462	0.1130	0.1027
30	0.1573	0.1025	0.0783	0.0709
40	0.1228	0.0789	0.0599	0.0541
50	0.1008	0.0641	0.0485	0.0438

Table: 3.4 The Kinetic Parameters for the Adsorption of Cr (VI) ion onto ASI-NC

C <sub>0</sub>	Temp °C	Pseudo Second Order				Elovich Model			Intraparticle Diffusion		
		q <sub>e</sub>	k <sub>2</sub>	γ	H	α	β	γ	K <sub>id</sub>	γ	C
10	30	19.702	0.0035	0.9834	1.3455	30.505	0.2497	0.9925	0.1083	0.9829	1.3546
	40	18.476	0.0098	0.9835	3.3521	114.220	0.4787	0.9853	0.1344	0.9821	1.6888
	50	18.459	0.0166	0.9891	5.6543	655.70	0.7172	0.9855	0.0840	0.9849	1.7929
	60	18.463	0.0177	0.9861	6.0282	128.98	0.7557	0.9865	0.0792	0.9859	1.8029
20	30	36.533	0.0035	0.9895	4.6167	51.924	0.2003	0.9908	0.1717	0.9881	1.6000
	40	36.784	0.0039	0.9842	5.2116	77.498	0.2097	0.9863	0.1599	0.9849	1.6302
	50	37.142	0.0044	0.9875	6.0544	125.093	0.2200	0.9858	0.1481	0.9874	1.6626
	60	37.642	0.0049	0.9837	6.9978	297.326	0.2427	0.9875	0.1293	0.9891	1.7062
30	30	49.657	0.0037	0.9845	9.1898	707.665	0.1997	0.9912	0.1179	0.9832	1.6683
	40	51.383	0.0041	0.9902	10.737	574.804	0.1837	0.9854	0.1237	0.9823	1.6805
	50	53.405	0.0034	0.9887	9.813	242.394	0.1576	0.9876	0.1419	0.9815	1.6613
	60	53.018	0.0050	0.9903	14.032	110.493	0.1856	0.9855	0.1168	0.9817	1.7161
40	30	65.591	0.0037	0.9878	15.877	565.467	0.1362	0.9892	0.1306	0.9836	1.6578
	40	67.085	0.0035	0.9836	15.586	570.787	0.1336	0.9869	0.1306	0.9845	1.6657
	50	67.732	0.0037	0.9867	16.985	784.784	0.1369	0.9916	0.1252	0.9865	1.6819
	60	68.692	0.0037	0.9898	17.478	898.050	0.1370	0.9872	0.1231	0.9876	1.6921
50	30	77.610	0.0022	0.9845	13.063	508.522	0.1162	0.9874	0.1317	0.9863	1.6128
	40	78.658	0.0021	0.9904	13.177	505.672	0.1145	0.9867	0.1321	0.9884	1.6178
	50	78.830	0.0023	0.9839	14.227	832.045	0.1212	0.9874	0.1230	0.9832	1.6377
	60	80.576	0.0021	0.9862	13.630	576.259	0.1133	0.9903	0.1299	0.9832	1.6324

Table: 3.5 Thermodynamic Parameter for the Adsorption of Cr (VI) ion onto ASI-NC

C <sub>0</sub>	ΔG°				ΔH°	ΔS°	E <sub>a</sub>	S*
	30°C	40°C	50°C	60°C				
10	-3639.3	-4706.2	-5456.8	-5695.5	17.458	70.229	14887.8	0.0005
20	-3987.1	-4354.7	-4744.7	-5504.6	10.915	48.938	9332.26	0.0043
30	-3150.0	-3548.7	-4067.0	-4416.6	9.9544	43.239	8018.14	0.0092
40	-2963.1	-3339.6	-3612.2	-3927.5	6.6325	31.739	5207.95	0.0296
50	-2465.3	-2666.1	-2828.3	-3130.4	4.0491	21.452	3001.47	0.0834

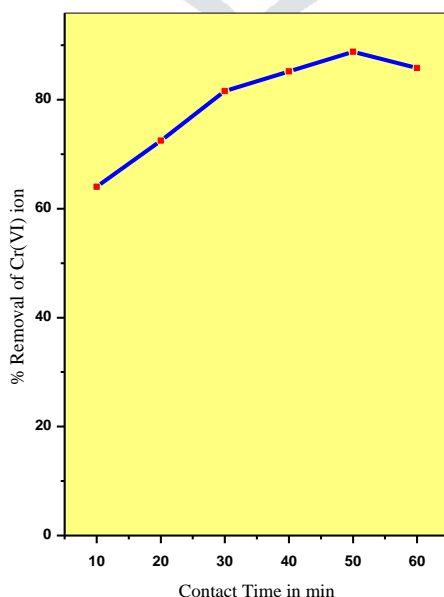
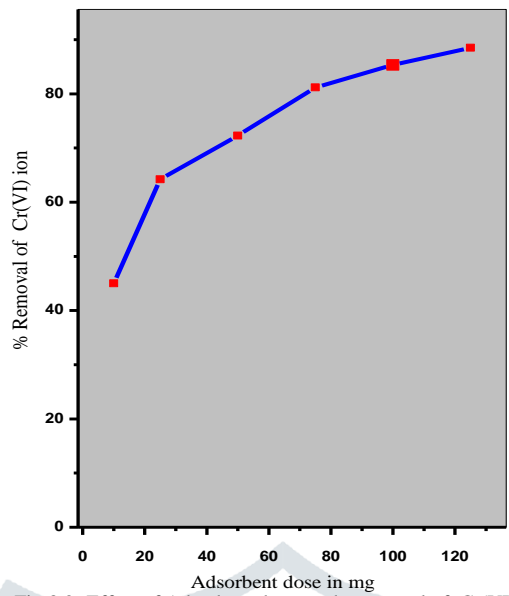
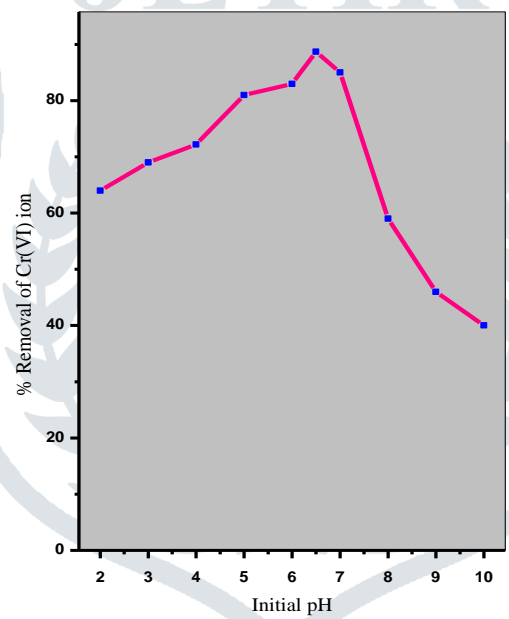


Fig:3.1- Effect of Contact Time on the Removal of Cr(VI) ion  
[Cr(VI)]=50 mg/L; Temperature 30°C; Adsorbent dose=0.025g/50ml



Fig;3.2- Effect of Adsorbent dose on the removal of Cr(VI) ion  
 [Cr(VI)]=20mg/L;Contact Time 45 min;Temprature 30°C



Fig;.3.3- Effect of Initial pH on the removal of Cr(VI) ion  
 [Cr(VI)]=20mg/L;Temprature 30°C;Adsorbent dose=0.025g/50ml